



# Near-edge elastic photon scattering in amorphous systems

R.P. Hugtenburg<sup>a,b,\*</sup>, D.W. England<sup>b</sup>, D.A. Bradley<sup>c</sup>

<sup>a</sup> School of Physics and Astronomy, University of Birmingham, B15 2TT, UK

<sup>b</sup> Queen Elizabeth Medical Centre, University Hospital Birmingham, B15 2TH, UK

<sup>c</sup> Department of Physics, School of Electronics & Physical Sciences, University of Surrey, GU2 7XH, UK

Available online

## Abstract

The structure of valence and unoccupied electron orbitals and the neighbouring electron density distribution of atoms and ions in amorphous systems can be examined through use of resonance in the elastic photon scattering-cross-section in the vicinity of core atomic orbital energies. So-called anomalous X-ray scattering (AXS) is a mode of analysis that offers similar information to that of EXAFS but can be obtained concurrently with diffraction mode imaging. Of interest is whether the dilute-ion aqueous system provides an environment suitable for testing independent particle approximation (IPA) predictions. With the aqueous environment as the reference system for calibrating relative cross-sections, particular challenges include photons scattered by the medium being subsequently absorbed by the ion, limiting the thickness of the attenuating medium and motivating use of bright synchrotron photon sources where tunable X-rays are obtained at sub-eV resolution using a Si 111 monochromator. Measured scattering intensities and fluorescent yields were compared and shown to agree qualitatively with Monte Carlo calculations utilising amplitudes calculated from modified form-factors with anomalous scatter factors at a resolution of several eV determined from the Dirac–Slater exchange potential. Experimentally determined form-factors for pure water were used to calibrate fluorescent yield and elastic scattering intensities for measurement of the energy dependent variation of these quantities near edge and XRF imaging of the Zn concentration in wax mounted, formalin fixed, breast tumour samples. Results indicate the distribution of Zn at higher resolution than sampling dimensions used in previous studies. Shifts in the position and profile of *K*-edge absorption and elastic scattering features in aqueous Zn, Zn doped sol–gel glass and Zn in tissue are shown to reflect changes in the atomic charge state and environment and offer support for the presence of non-nutrient Zn bearing components at elevated concentrations in tumour, of which the matrix-metalloprotein MMP-II is a likely contender.

© 2007 Elsevier B.V. All rights reserved.

PACS: 32.80.Cy; 87.54.Gb

Keywords: Anomalous scattering; Near-edge; Trace elements

## 1. Introduction

X-ray fluorescence (XRF) and anomalous elastic scattering (AXS) [1] offer complementary information that can be used to determine elemental abundances as well as charge state and environment of trace constituent atoms in biological systems. Synchrotron based XRF (e.g. micro-SXRF) currently offers high resolution mapping of

the concentration of trace elemental components in samples and, in particular, provides a new window on biological systems involving metals. Through the dispersion effect, variation in the absorption cross-section leads to scattering interference terms that are characterised by rapid variation in the elastic scattering signal close to the atomic orbital edges. We consider the impact of calibration methods used in XRF, diffraction enhanced imaging (DEI) and species and environment sensitive scattering techniques such as AXS where, with increasing synchrotron brightnesses, high resolution atom and environment specific mapping is fast become a reality.

\* Corresponding author. Address: School of Physics and Astronomy, University of Birmingham, B15 2TT, UK

E-mail address: [r.p.hugtenburg@bham.ac.uk](mailto:r.p.hugtenburg@bham.ac.uk) (R.P. Hugtenburg).

While previous direct measurements of elastic scattering cross-sections have achieved high degrees of precision, either utilising gamma-ray sources scattering in solid metallic systems [2] or synchrotron light scattering in dual cells containing noble gases [3], this work focuses on the validity of the independent particle approximation (IPA) for a variety of atoms and ions embedded in amorphous systems that typify the biological context [4–6]. In this current work we examine Zn embedded in variety of target systems ranging from vapour deposited metallic Zn coatings on glass, in which IPA assumptions are expected to be invalid due to significant inter-atomic correlation but for which the standard tabulated data, including the binding energy for the atom, are determined; to Zn doped sol–gel glass where the structure is essentially amorphous but nearest neighbour effects are dominated by a Zn–O covalent bond; to the aqueous environment where the nearest neighbour to the Zn 2+ ion is a loosely bound oxygen through the high electronegativity associated with O in the water molecule. Calculations of cross-sections within IPA, such as the anomalous scattering factor (ASF) approach, are required at high resolution, and the more computationally intensive *S*-matrix calculation is excluded in the present study.

Recent synchrotron based XRF analysis of trace elements in cancerous human tissue has demonstrated elevated concentrations of metals such as Zn in regions that are identified as tumour [7,8]. Changes in the nutrient supply can explain some of the noted increases but could be due to the formation of the Zn bearing matrix-metalloprotein, MMP-II, a gelatinase, which has been associated with the infiltration of tumour into normal tissue (metastasis). X-ray absorption near edge spectroscopy (XANES) is used to determine the charge state of Zn in tissue through analysis of the shift in the ionisation threshold due to the increased overall charge seen by perturbed electrons and variations in bound–bound transitions occurring just below the ionisation threshold. Likewise, the elastic scattering cross-section changes near edge exhibiting shifts in the position of the elastic scattering minimum, as well as adjustments in the absolute value of the cross-section. We examine the variation of the concentration of Zn via XRF at higher resolution than previously recorded. XANES mode imaging is also used to determine the speciation of the Zn detected. It is anticipated that differences between XANES spectra obtained for aqueous Zn 2+ ions and tissue are indicative of non-nutrient, covalently bonded, Zn where comparisons are drawn with the additional model, Zn doped sol–gel glass, which exhibits covalent bonding [9,10].

## 2. Methods

At BM28 (XMAS, ESRF), tunable X-rays at eV resolution are obtained by passing the white light spectrum of the 3rd generation (6 GeV) synchrotron source through a dual 111 Si monochromator. X-rays were scattered through high angle from aqueous Zn solutions with concentrations

ranging from 0.01 to 1 mol l<sup>-1</sup> which were contained in an optically thick perspex cell provided with 8 μm Kaplan windows. High scattering angles are used to minimise the effect of diffraction in the medium and optical path-length, however discrepancies between the form-factor approximation and the more rigorous *S*-matrix calculation are known to increase with angle. Cross-sections computed from *S*-matrix calculations are found to be just 0.5% smaller for neutral Zn in this energy range [2] but have yet to be determined at the high energy resolution required near edge.

Scattering was detected by a HPGe detector where energy resolution of ~500 eV was adequate to separate the elastic scattering signal from K-alpha radiation but not from Compton or K-beta contributions. The Compton contribution from the medium was removed assuming the validity of the relativistic impulse approximation. The contribution due to K-beta fluorescence was handled by assuming the branching ratio for K-alpha and K-beta contributions to be constant. The combined K-alpha and K-beta fluorescence was monitored with a silicon drifted detector (SDD, Roentec) placed at a 90° angle to the incoming beam in the plane of the electron storage ring.

ASF and modified form-factor (MFF) amplitudes are computed for a Dirac–Slater exchange potential utilising the RTAB Rayleigh scattering library codes [11] for calculations of positive ions [12]. Complex coupling of attenuation and scattering of the outgoing signal, including multiple scattering, were handled with the Monte Carlo code XRFCOMP [13] which is an amalgam of the EGS4 [14] and LSCAT [15,16] libraries specialized for the XRF application.

The analysis was extended from the aqueous system to wax mounted, formalin fixed tissue samples of breast tumours resected for therapeutic purposes. A motorised stage was used to scan the sample through a beam of 0.15 mm × 0.133 mm aperture size. With the sample oriented at 45° in two axes with respect to the beam axis, the footprint on the sample was 0.189 mm × 0.211 mm. Tissue types within the sample were identified with the assistance of a histopathologist.

## 3. Results

Measured scattering intensities are comprised principally of elastic scattering in the medium. Scattering in the target atom however leads to a clearly observable minimum in the ratio of the elastic scattering intensity of the aqueous Zn solution where variations in the intensity ratio with angle of incidence accord with Monte Carlo calculations to within 5%, including the loss of sensitivity at low angles of incidence where absorption dominates. The intensity ratio at the minimum for the two high angle measurements correspond to a value of the angle independent ASF amplitude  $f'$  of  $-8 + / - 2$  eu/atom compared with  $-10$  eu/atom predicted for Zn 2+ ion where the contribution to the amplitude from bound–bound transitions has been Lorentz

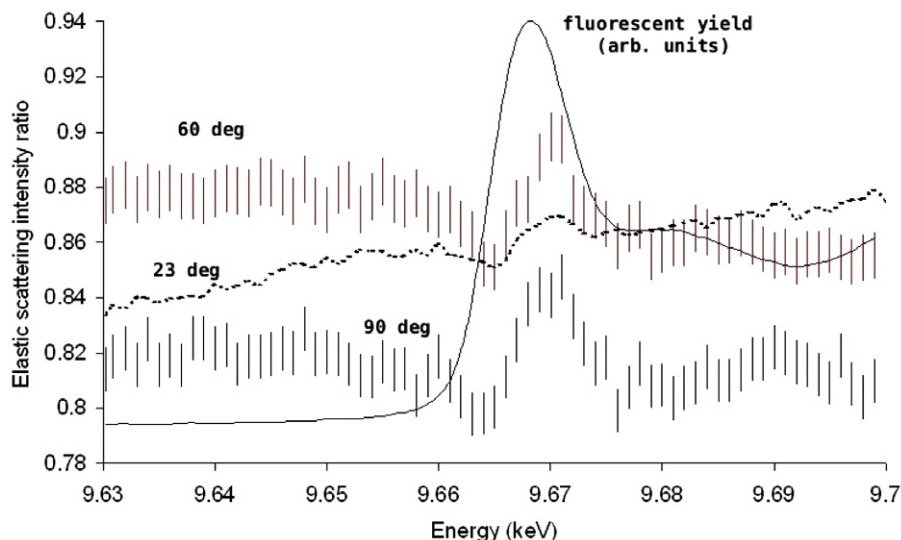


Fig. 1. Intensity of scattered X-rays, including elastically scattered photons from the Zn 2+ ion from aqueous Zn(NO<sub>3</sub>)<sub>2</sub> (1 mol l<sup>-1</sup>) and in the water medium relative to scattering in pure water for angles for 90°, 60° and 23° scattering where the final case was of substantially diminished quality and where K-beta fluorescence and resonant Raman scattering are removed in proportion to the variation in the K-alpha line. The predicted minimum due to elastic scattering in the target is clearly observed and corresponds to the binding energy according to its assignment as the first point of inflection in the rising absorption cross-section shown in the fluorescent yield.

broadened by 3 eV and otherwise achieves good qualitative agreement with absorption and scattering profiles. The uncertainty in the measured cross-section is 5% whereas ASF and *S*-matrix have previously been shown to agree to within 1% (Fig. 1).

Fig. 2 shows sub-mm variation in the fluorescent yield of Zn in wax-mounted tumour-bearing breast tissue. Maximum concentrations of Zn exceed those reported in earlier studies [7,8] due to apparent heterogeneity in the distribution of Zn observed at the higher resolutions used in this

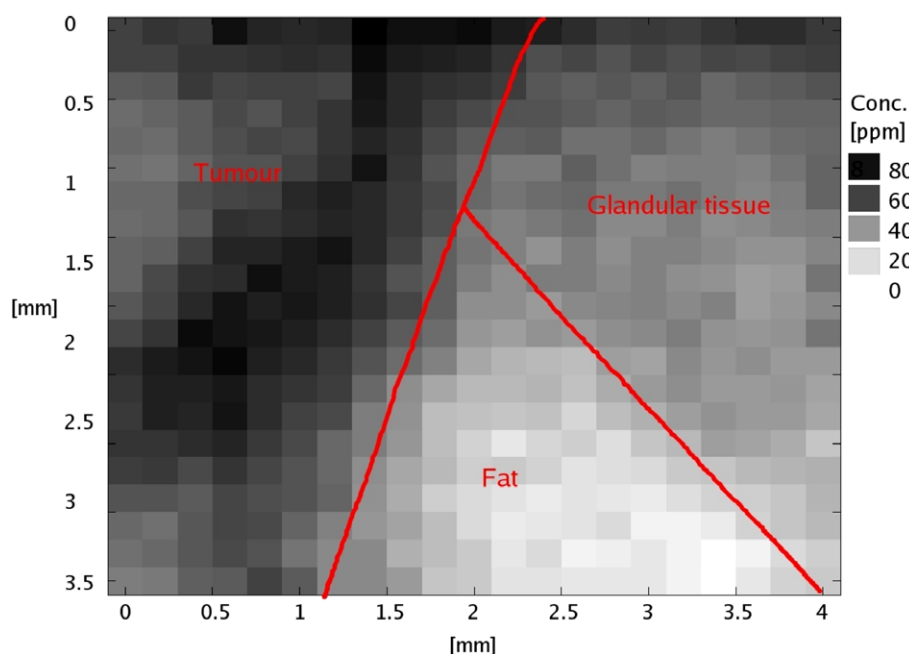


Fig. 2. Distribution of Zn in a 3.97 mm × 4.43 mm section of tissue identified as bearing tumour, adipose (principally fat) and glandular material by measuring fluorescence in the sample through 9.65 keV monochromatic X-rays at a 21 × 21 raster of points using a 0.15 mm × 0.133 mm source aperture. Fluorescent photons were recorded in a high count rate silicon drifted detector (Roentec) placed close to the sample at 90° to the direction of incidence in the plane of the electron orbit. The high degree of polarisation in the ESRF synchrotron storage ring ensures a small background (<2%) of scattered photons at the detector that are principally multiple scattering processes in the sample.

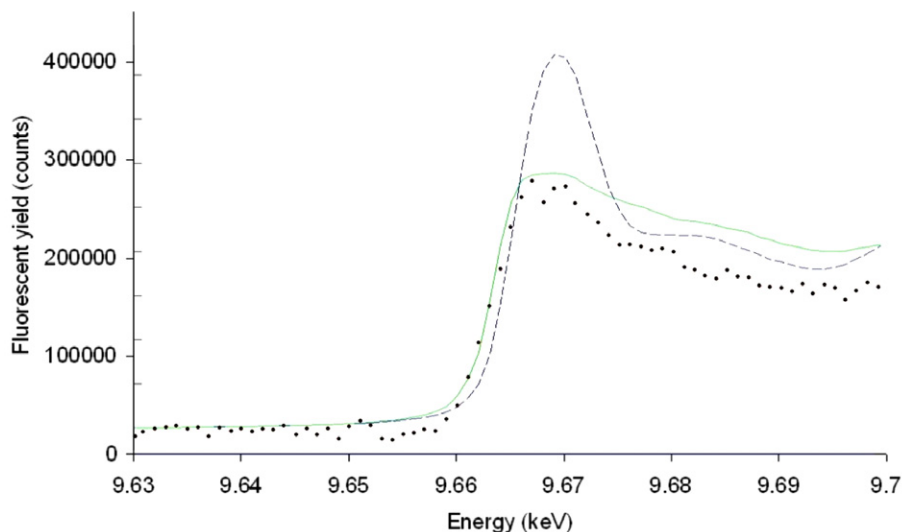


Fig. 3. X-ray absorption near edge spectra (XANES) for aqueous Zn  $2+$  ions ( $\text{Zn}(\text{NO}_3)_2$ , dashed line), Zn doped sol-gel silica glass (solid line) and tumour bearing tissue (points). The shift in the absorption threshold due to increased charge state (chemical shift) for Zn  $2+$  ions relative to the edge for neutral Zn (9.659 keV) is 8 eV smaller than IPA predictions from a Dirac–Slater exchange potential which is likely to be mostly due to inter-atomic effects in the neutral species.

study. Further, the Zn is shown in this and repeat scans with other tumour to be concentrated substantially on the periphery of the tumour region. A comparison of XANES spectra for Zn ions in aqueous solution, sol-gel glass and tumour (Fig. 3) supports the contention that a large component of Zn is non-nutrient (i.e. not aqueous Zn  $2+$ ) and perhaps associated with the presence of MMP-II. Close agreement between the profiles of XANES spectra for Zn-doped glass and tumour bearing tissue support comparisons with modelled profiles limit the proportion of aqueous Zn  $2+$  within the tissue to less than 10% of the total Zn.

#### 4. Conclusion

Direct measurements of the elastic scattering signals from Zn ions in aqueous solution at a range of angles and concentrations clearly demonstrate the sharp feature associated with the rapid variation in the complementary anomalous scattering factors in the vicinity of the K-shell absorption-edge. The elastic scattering minimum for Zn  $2+$  ions corresponds to a value of  $f' = -10$  eu/atom, calculated with 3 eV Lorentz broadening. Monte Carlo simulation of this experiment indicates an amplitude for  $f'$  that is  $2 \pm 2$  eu/atom larger than that determined within IPA which corresponds to a 5% discrepancy with calculated cross-sections. While some aspects of the method offer high analytical power, for example the concentration of solute which can be controlled through titration, significant errors remain unaccounted for, including the assumption of the flatness of the liquid cell surface. The advantage of the aqueous environment is that it provides a sounder basis for IPA assumptions. This is illustrated through a greatly diminished environmental electron density in the aqueous

system where the average Zn–O bond length is 0.210 nm with an 8-fold coordination [17] compared to 0.104 for Zn-doped glass with 8-fold coordination [10].

The imaging used in this study demonstrates the need to sample variation in Zn concentrations between tissues and donors at higher spatial resolution. Further, the spectrographic methods such as XANES that can be used in conjunction with synchrotron XRF offer new information about the nature of Zn found in association with tumour, including a predominately covalent state pointing to Zn bearing matrix-metalloprotein MMP-II. The results of this study therefore suggest that an imaging method that combines fluorescence with small-angle elastic scattering could be a sensitive probe of malignancy, either primary or metastatic, thus providing valuable data to both surgeon and oncologist prior to treatment.

#### Acknowledgements

This work was performed on the EPSRC-funded *XMaS* beam line at the ESRF. We appreciate the support of the Department of Histopathology at University Hospital Birmingham.

#### References

- [1] Y. Waseda, Springer Tr. Mod. Phys. 179 (2002).
- [2] D.A. Bradley, S.C. Roy, L. Kissel, R.H. Pratt, Radiat. Phys. Chem. 56 (1999) 175.
- [3] L. Young, R.W. Dunford, E.P. Kanter, et al., Phys. Rev. A 63 (10) (2001) 052718.
- [4] R.P. Hugtenburg, P. Muthuvelu, D.A. Bradley, Phys. Med. Biol. 47 (2002) 3407.
- [5] R.P. Hugtenburg, D.A. Bradley, Nucl. Instr. and Meth. B 213 (2004) 552.

- [6] R.P. Hugtenburg, A.L. Yusoff, D.A. Bradley, *Phys. Chem.* 71 (2004) 655.
- [7] K. Geraki, M.J. Farquharson, D.A. Bradley, *Phys. Med. Biol.* 47 (2002) 2327.
- [8] K. Geraki, M.J. Farquharson, D.A. Bradley, R.P. Hugtenburg, *Nucl. Instr. and Meth. B* 213 (2004) 564.
- [9] A.L. Yusoff, R.P. Hugtenburg, D.A. Bradley, *Radiat. Phys. Chem.* 71 (2004) 887.
- [10] A.L. Yusoff, R.P. Hugtenburg, D.A. Bradley, *Radiat. Phys. Chem.*, in press.
- [11] L. Kissel, *Radiat. Phys. Chem.* 59 (2000) 185.
- [12] B. Zhou, L. Kissel, R.H. Pratt, *Nucl. Instr. and Meth. B* 66 (1992) 307.
- [13] R.P. Hugtenburg, J.R. Turner, D.M. Mannering, B.A. Robinson, *Appl. Rad. Isot.* 49 (1998) 673.
- [14] W.R. Nelson, H. Hirayama and D.W.O. Rogers, SLAC Report 265, Stanford Linear Accelerator Center, Stanford, CA, 1985.
- [15] Y. Namito, S. Ban, H. Hirayama, *Nucl. Instr. and Meth. A* 332 (1993) 277.
- [16] Y. Namito, S. Ban, H. Hirayama, *Nucl. Instr. and Meth. A* 349 (1994) 489.
- [17] E. Matsubara, Y. Waseda, *J. Phys.: Condens. Matter* 1 (1999) 8575.